



Published in final edited form as:

*Kidney Int.* 2022 January ; 101(1): 79–91. doi:10.1016/j.kint.2021.09.033.

## Myeloid cyclooxygenase-2/prostaglandin E2/E-type prostanoid receptor 4 promotes transcription factor MafB-dependent inflammatory resolution in acute kidney injury:

### PGE2 modulates macrophage phenotype through MafB

Yu Pan<sup>1,2,4,5</sup>, Shirong Cao<sup>1,2,5</sup>, Andrew S. Terker<sup>1,2</sup>, Jiaqi Tang<sup>1,2</sup>, Kensuke Sasaki<sup>1,2</sup>, Yinqiu Wang<sup>1,2</sup>, Aolei Niu<sup>1,2</sup>, Wentian Luo<sup>1,2</sup>, Xiaofeng Fan<sup>1,2</sup>, Suwan Wang<sup>1,2</sup>, Matthew H. Wilson<sup>1,2</sup>, Ming-Zhi Zhang<sup>1,2</sup>, Raymond C. Harris<sup>1,2,3</sup>

<sup>1</sup>Division of Nephrology and Hypertension, Department of Medicine, Vanderbilt University School of Medicine, Nashville, Tennessee

<sup>2</sup>Vanderbilt Center for Kidney Disease, Vanderbilt University School of Medicine, Nashville, Tennessee

<sup>3</sup>Department of Veterans Affairs, Nashville, Tennessee

<sup>4</sup>Division of Nephrology, Shanghai Ninth People's Hospital, Shanghai Jiao Tong University School of Medicine

<sup>5</sup>These authors contributed equally.

### Abstract

Following acute injury to the kidney, macrophages play an important role in recovery of functional and structural integrity, but organ fibrosis and progressive functional decline occur with incomplete recovery. Pro-resolving macrophages are characterized by increased cyclooxygenase 2 (COX-2) expression and this expression was selectively increased in kidney macrophages following injury and myeloid-specific COX-2 deletion inhibited recovery. Deletion of the myeloid prostaglandin E2 (PGE2) receptor, E-type prostanoid receptor 4 (EP4), mimicked effects seen with myeloid COX-2<sup>-/-</sup> deletion. PGE2-mediated EP4 activation induced expression of the transcription factor MafB in kidney macrophages, which upregulated anti-inflammatory genes and suppressed pro-inflammatory genes. Myeloid MafB deletion recapitulated the effects seen with either myeloid COX-2 or EP4 deletion following acute kidney injury, with delayed recovery, persistent presence of pro-inflammatory kidney macrophages, and increased kidney fibrosis.

**Correspondence:** Dr. Raymond C. Harris, C-3321 Medical Center North, Department of Medicine, Vanderbilt University School of Medicine, Nashville, TN 37232. Tel#: 615-322-2150, ray.harris@vumc.org Or Dr. Ming-Zhi Zhang, S3223 Medical Center North, Department of Medicine, Vanderbilt University School of Medicine, Nashville, TN 37232. ming-zhi.zhang@vumc.org.

**Author Contributions:** M-ZZ and RCH conceived the study, YP, SC, AST, KS, YW, AN, WL, MHW, XF and SW performed the experiments, YP, M-ZZ and RCH wrote the manuscript, YP, SC, M-ZZ and RCH prepared the figures and edited the manuscript. We thank Dhousha Daassi for fruitful discussions.

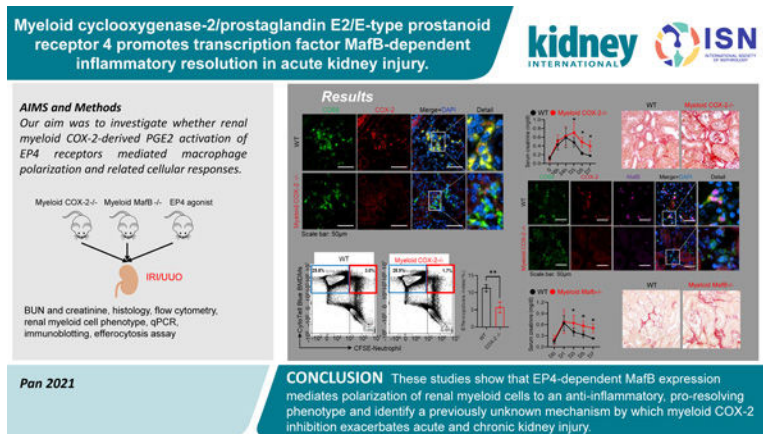
**Publisher's Disclaimer:** This is a PDF file of an unedited manuscript that has been accepted for publication. As a service to our customers we are providing this early version of the manuscript. The manuscript will undergo copyediting, typesetting, and review of the resulting proof before it is published in its final form. Please note that during the production process errors may be discovered which could affect the content, and all legal disclaimers that apply to the journal pertain.

Disclosure

There is nothing to disclose.

Thus, our studies identified a previously unknown mechanism by which prostaglandins modulate macrophage phenotype following acute organ injury and provide new insight into mechanisms underlying detrimental kidney effects of non-steroidal anti-inflammatory drugs that inhibit cyclooxygenase activity.

## Graphical Abstract



## Translational Statement

The mammalian kidney is easily injured by ischemic or toxic insults but can often recover functional and structural integrity. Innate immunity is involved in both the injury and recovery processes. During resolution from injury, renal myeloid cells express increased cyclooxygenase 2 (COX-2), and myeloid COX-2 deletion delayed renal recovery from acute kidney injury. These studies report the mechanism by which myeloid COX-2 signaling induces polarization of tissue macrophages to a pro-resolving phenotype via EP4-mediated MafB activation and identify a previously unknown mechanism underlying detrimental effects of cyclooxygenase inhibition by nonsteroidal antiinflammatory drugs in the setting of renal dysfunction.

## Keywords

Cyclooxygenase 2; macrophage polarization; AKI; renal fibrosis

## Introduction

Acute kidney injury (AKI) is defined as an abrupt decrease in renal function. The incidence of AKI varies from 5% in all hospitalized patients to 30%–50% in intensive care units<sup>1</sup>. Incomplete recovery from AKI leads to chronic kidney disease. As the majority of interventional trials in AKI have failed in humans, novel therapeutic approaches are needed to prevent or treat AKI. There is increasing evidence for an important role for innate immune cells in propagation of AKI<sup>2–4</sup>. In addition, following the acute influx of proinflammatory myeloid cells, there is a shift from a proinflammatory to an antiinflammatory and pro-resolution phenotype, which mediates repair and resolution of

the injury. Failure to produce effective resolution following AKI can lead to incomplete recovery and progressive tubulointerstitial fibrosis.

Arachidonic acid metabolites result from metabolism by three distinct enzymatic pathways: the cyclooxygenase, lipoxygenase and CYP450 pathways. Cyclooxygenase (COX) is the rate-limiting enzyme that metabolizes arachidonic acid to prostaglandin G2 and subsequently to prostaglandin H2, thereby serving as the precursor for subsequent metabolism by prostaglandin and thromboxane synthases. Two isoforms of COX exist in mammals, constitutive COX-1 and inducible COX-2. COX metabolites have pleiotropic functions, mediated by specific G-protein coupled receptor signaling. The most prevalent prostanoid is PGE2, which signals through four distinct G protein coupled receptors- EP1 through EP4. EP1 is coupled primarily to G<sub>q</sub>/G<sub>11</sub> and EP3 to G<sub>i</sub>, while EP2 and EP4 are primarily coupled to G<sub>s</sub>. Depending upon the tissue distribution of specific PGE2 receptors, PGE2 may act as either a pro- or an antiinflammatory mediator. COX-2 is expressed in renal immune cells, particularly renal monocytes/macrophages. EP4 is the predominant PGE2 receptor in macrophages<sup>5</sup>, and previous studies have demonstrated that EP4 activation in macrophages inhibits macrophage proinflammatory cytokine and chemokine release<sup>5-8</sup>.

The myeloid cell COX-2 response to ischemic AKI has not been previously investigated. In addition, the potential roles of renal myeloid cell COX-2, COX-2-derived PGE2, and PGE2 receptors in renal macrophage polarization, in the initiation and propagation and recovery of renal structural integrity and function following ischemic AKI have not been investigated. In the current studies, we found that renal COX-2 was selectively increased in renal macrophages after ischemic injury. Renal macrophage COX-2-dependent activation of myeloid EP4 induced the transcription factor MafB to promote macrophage polarization to an antiinflammatory and pre-resolving phenotype, facilitating recovery from acute injury and protecting against the development of subsequent renal fibrosis.

## Materials and Methods

### Animals.

All animal experiments were performed in accordance with the guidelines of the IACUC of Vanderbilt University. COX-2<sup>-/-</sup> mice were on C57BL/6 background. EP4<sup>f/f</sup> mice were generated in Dr. Breyer's laboratory<sup>9</sup>, COX-2<sup>f/f</sup> mice in Dr. Fitzgerald's laboratory<sup>10</sup>, CD11b-Cre mice in Dr. Vacher's laboratory<sup>11</sup>, and all mice were backcrossed onto the FVB background for 12 generations. Myeloid COX-2<sup>-/-</sup> mice (CD11b-Cre; COX-2<sup>f/f</sup>) and wild-type (WT) mice (COX-2<sup>f/f</sup>) as well as myeloid EP4<sup>-/-</sup> mice (CD11b-Cre; EP4<sup>f/f</sup>) and WT mice (EP4<sup>f/f</sup>) were used. C57BL/6 Mafb<sup>tm1.1 mrl</sup> (10621) were from Taconic laboratory and C57BL/6J LysM-Cre mice (004781) were from Jackson laboratory (Bar Harbor, ME), and myeloid Mafb<sup>-/-</sup> (LysM-Cre; Mafb<sup>f/f</sup>) mice and WT (Mafb<sup>f/f</sup>) mice were generated. Male, 8-10 weeks old mice were used for all experiments and genotypes were confirmed with PCR before and after experiments. The primers used are described in Supplementary Materials and Methods.

### Antibodies and reagents.

A full list of antibodies is shown in Table S2. PGE2 and CAY10598 (EP4 agonist) were from Cayman Chemical; PF04418948 (EP2 antagonist), L161982 (EP4 antagonist), H-89 (PKA inhibitor), 6-Bnz-cAMP (PKA agonist), 666–15 (CREB inhibitor), and dibutyryl-cAMP (analog of cAMP) were from TOCRIS for *in vitro* study.

### Ischemic AKI and UUO and EP4 agonist administration.

Ischemia-reperfusion-induced AKI was carried out as previously described<sup>2</sup>. Briefly, the animals were uninephrectomized, immediately followed by unilateral ischemia-reperfusion with renal pedicle clamping for 32 min. For UUO, unilateral ureter was ligated for 7 days, and the EP4 agonist, ONO-4819 (rivenprost, Cayman Chemicals) was given to a subgroup of each of the myeloid knockout mice via 2004 minipump (Alzet) at a dose of 75 µg/kg/day one day before surgery.

### Isolation of BMDMs and renal myeloid cells.

BMDMs were isolated using a monocyte isolation kit for mice (Miltenyi Biotec, 130–100-629). Renal myeloid cells were enriched using mouse CD11b Microbeads and MACS columns (Miltenyi Biotec Auburn, CA) following the manufacturer's protocol. The purity of renal myeloid cells isolated with CD11b Microbeads was >95% ( $95.34 \pm 2.04$ , n=4), as determined by flow cytometry (CD45<sup>+</sup> CD11b<sup>+</sup> cells). For *ex vivo* polarization, an M0 phenotype was achieved by culturing BMDMs in DMEM for 48 h, an M1 polarization by culturing with LPS and IFN-γ (1 µg/ml for each) for 24 h, and an M2 polarization by culturing with IL-4 and IL-13 (10 ng/ml for each) for 48 h.

### Flow cytometry analysis.

Kidney single cell suspensions were prepared according to previous reports<sup>12</sup>. Cells were incubated in 2.5 µg/ml Fc blocking solution, centrifuged (300x g, 10 min, 4°C) and resuspended with FACS buffer. Cells were stained for 60 min at 4°C with fluorescent conjugated antibodies against different cell marker antigens (Table S2) or isotype control. A total of 50 000–1 00 000 cells were acquired by scanning using NovoCyte Quanteon Flow Cytometer Systems. Cell debris and dead cells were excluded from the analysis based on scatter signals and use of Zombie Violet™ Fixable Viability Kit (Biolegend, Cat# 423114). For efferocytosis analysis, neutrophils isolated with anti-Ly-6G microbeads (130–120-337, Miltenyi) from WT bone marrows were stained with CFSE and treated with Staurosporine (1:1000) for 2 h at 37°C to induce apoptosis. BMDMs isolated from WT, myeloid COX-2<sup>-/-</sup>, and myeloid Mafb<sup>-/-</sup> mice were stained with CytoTell™ blue. A mixture of labeled apoptotic neutrophils and BMDMs (4:1) were cultured at 37°C for 6 h. For detection of efferocytosis, cells were gated on CytoTell™ blue positivity before counting the number of events that were also CFSE positive.

### Cyclooxygenase activity assay.

BMDMs were suspended in 2 ml RPMI1640 containing 60 µM arachidonic acid and incubated for 1 h at 37°C. Medium was harvested for prostanoid measurement by gas chromatographic/negative ion chemical ionization mass spectrometric assays (GC/MS)

using stable isotope dilution<sup>13</sup>. Protein concentration was measured using protein assay kit from Bio-Rad. The production of metabolites is expressed as ng/mg/min in BMDMs.

#### **Quantitative immunofluorescence/immunohistochemistry staining.**

Kidney tissue was immersed in fixative containing 3.7% formaldehyde, 10 mM sodium m-periodate, 40 mM phosphate buffer, and 1% acetic acid. The tissue was dehydrated through a graded series of ethanols, embedded in paraffin, sectioned (4  $\mu$ m), and mounted on glass slides. Immunostaining was carried out as in previous reports<sup>14</sup>. Antigen retrieval in the deparaffinized sections was performed with citrate buffer by microwave heat for 10 min and the slides were then blocked with 10% normal donkey serum for 1 h followed by incubation with primary antibodies overnight at 4°C. For double immunofluorescence staining, the sections were incubated in two rounds of staining overnight at 4°C. Anti-rabbit or mouse IgG-HRP were used as secondary antibodies (Santa Cruz). Each round was followed by tyramide signal amplification with the appropriate fluorophore (Alexa Fluor 488 tyramide, Alexa Fluor 647 tyramide or Alexa Fluor 555 tyramide, Tyramide SuperBoost Kit with Alexa Fluor Tyramides, Invitrogen) according to its manufacturer's protocols. DAPI was used as a nuclear stain. Sections were viewed and imaged with a Nikon TE300 fluorescence microscope and spot-cam digital camera (Diagnostic Instruments), followed by quantification using Image J software (NIH, Bethesda, MD). IOD were calculated in more than 30 fields per mouse or 10 fields per cell slide and expressed as arbitrary units or percentage of per field by two independent investigators.

Immunoblotting analysis, efferocytosis assay, qPCR, establishment of Mafk knockout cell lines, and luciferase promoter activity assay were described in Supplementary Materials and Methods.

#### **Kidney TNF- $\alpha$ measurement.**

Mouse TNF- $\alpha$  DuoSet ELISA kit (Catalog No. DY410-05) was used to measure kidney TNF- $\alpha$  levels in accordance with the manufacturer's instructions (R&D Systems).

**Picro-Sirius red stain** was performed according to the protocol provided by the manufacturer (Sigma, St. Louis, MO, USA).

#### **Measurement of BUN and serum creatinine.**

BUN was measured using a Urea Assay Kit (BioAssay Systems, Hayward, CA). Quantification of endogenous creatinine was performed on an ultra-performance liquid chromatography (UPLC) tandem mass spectrometry system as previously described<sup>15</sup>.

#### **Bioinformatic data analysis.**

SRA documents were downloaded from the GEO database and converted into FASTQ on the Galaxy online system. All ChIP-seq data sets were aligned using Bowtie2 to build version mouse NCBI37/mm9 of the mouse genome<sup>16</sup>. ChIP-seq read densities in genomic regions were calculated. We used the MACS2 version peak calling with a p value  $< 1 \times 10^{-7}$  and a q value of less than 0.1 and a 2-fold enrichment threshold<sup>17</sup>. Bed files were analyzed with Bedtools and visualized alongside coverage files on IGV<sup>18</sup>. Gene set enrichment analysis

(GSEA) software were used to determine whether an *a priori* Maf<sup>b</sup> target gene set showed statistically significant concordant differences in BMDM with PGE<sub>2</sub> treatment<sup>19</sup>.

### Statistical analysis.

Data were expressed as the means  $\pm$  SD. The numeric data were analyzed using GraphPad Prism (version 9; GraphPad Software). Data were analyzed using 2 tailed Student's *t* test, one-way ANOVA, or two-way ANOVA followed by Tukey's or Bonferroni's post hoc tests. A *P* value less than 0.05 was considered significant. For each set of data, at least 4 different animals were examined for each condition. Collection, analysis, and interpretation of data were conducted by at least 2 independent investigators, who were blinded to the study.

## Results

### Renal COX-2 was selectively increased in renal macrophages after ischemic injury.

To determine the potential role of cyclooxygenase isoforms in the propagation and recovery after ischemic AKI, we first investigated the expression of COX isoforms, COX-1 and COX-2, in whole kidney and isolated renal myeloid cells after ischemic injury. *Ptgs1* (COX-1) mRNA levels in both total kidney and isolated renal myeloid cells decreased in the days following ischemic injury before returning toward baseline by day 7 (Fig. 1A). In contrast, renal myeloid cell *Ptgs2* (COX-2) mRNA levels markedly increased by day 3, when renal myeloid cells have begun to shift from a predominantly proinflammatory phenotype to a pro-resolving phenotype, although total kidney *Ptgs2* mRNA did not significantly change following ischemic injury (Fig. 1A). Of note, *Ptgs2* mRNA expression was about 100 times higher in renal myeloid cells than in corresponding total kidney tissue. Three days after ischemic AKI, increased renal COX-2 primarily colocalized with CD68+ cells, a marker of renal macrophages (Fig. 1B).

### Myeloid COX-2 deletion led to delayed recovery and increased kidney proinflammatory myeloid cells after ischemic injury.

We generated mice with selective COX-2 deletion in myeloid cells (CD11b-Cre; COX-2<sup>f/f</sup>; myeloid COX-2<sup>-/-</sup>) and utilized a model of ischemia-reperfusion kidney injury. In isolated renal myeloid cells 3 days after ischemic AKI, *Ptgs2* mRNA levels decreased >70% in myeloid COX-2<sup>-/-</sup> mice ( $1.52 \pm 0.49$  vs.  $5.12 \pm 1.08$  of WT mice,  $P < 0.01$ ) (Fig. 1C). Myeloid COX-2<sup>-/-</sup> mice and WT mice had similar initial injury, indicated by comparable BUN and serum creatinine levels at 16 and 24 h after injury (Fig. 1D). However, myeloid COX-2<sup>-/-</sup> mice had delayed functional recovery, indicated by slower decline of BUN and serum creatine levels (Fig. 1D). Additionally, immunofluorescent COX-2 was almost absent in CD68+ cells in myeloid COX-2<sup>-/-</sup> mice (Fig. 1B). We evaluated renal myeloid cell infiltration by flow cytometry (Fig. 1E). There were no differences in the renal macrophage or neutrophil populations between myeloid COX-2<sup>-/-</sup> mice and WT mice at baseline or one day after injury (Fig. 1F). However, at 3 days after ischemic injury, WT mouse kidney had decreased CD45<sup>+</sup>CD11b<sup>+</sup>Ly6G<sup>+</sup> neutrophils but persistently higher CD45<sup>+</sup>CD11b<sup>+</sup>F4/80<sup>+</sup> macrophages and further increased CD45<sup>+</sup>CD11b<sup>+</sup>Ly6C<sup>+</sup> monocytes. Of note, all of these myeloid subtypes were further increased in myeloid COX-2<sup>-/-</sup> mouse kidneys, with a



4-fold increased number of renal neutrophils in myeloid COX-2<sup>-/-</sup> mice compared to WT mice at day 3 after ischemic injury.

We recently reported that hematopoietic cell COX-2 polarizes skin macrophages to an antiinflammatory and pro-resolving phenotype<sup>20</sup>. Renal myeloid cell proinflammatory M1 cytokines/chemokines were comparable between WT mice and myeloid COX-2<sup>-/-</sup> mice under basal conditions. However, renal myeloid cell proinflammatory cytokines, *Tnf*, *Il23a*, *Ccl3* and *Nos2* (iNOS), were all significantly higher in myeloid COX-2<sup>-/-</sup> mice than WT mice at day 3 following ischemic injury (Fig. 1 G). ELISA and immunoblotting analysis confirmed higher kidney TNF- $\alpha$  and IL-6 protein levels in myeloid COX-2<sup>-/-</sup> mice at day 3 after ischemic injury (Fig. 1 H-I).

Efferocytosis, clearance of apoptotic neutrophils by macrophages, is critical in resolution of acute injury<sup>21</sup>. We found that renal macrophages isolated from myeloid COX-2<sup>-/-</sup> mice at 2 days after ischemic injury had decreased efferocytosis ability, indicated by decreased phagocytosis of apoptotic neutrophils (Fig. S1A). Flow cytometry analysis also demonstrated that COX-2<sup>-/-</sup> BMDMs had decreased efferocytosis of apoptotic neutrophils, indicated by the decreased ratio of phagocytic to non-phagocytic cells (Fig. S1B).

#### **Myeloid COX-2 deletion led to persistent renal inflammation and development of renal fibrosis 4 weeks after severe ischemic injury.**

Myeloid COX-2<sup>-/-</sup> mouse kidneys had persistently increased macrophages and proinflammatory cytokines (Fig. 2A and Fig. S2). Renal myeloid cells from myeloid COX-2<sup>-/-</sup> mice expressed higher levels of proinflammatory cytokines (Fig. 2B). Myeloid COX-2<sup>-/-</sup> mice had increased renal mRNA expression of profibrotic and fibrotic components, including *Acta2*, *Tgfb1*, *Ccn2/Ctgf*, *Colla1*, *Col3a1*, and *Fn* (Fig. 2C). Quantitative Sirius red staining, immunoblotting and immunostaining further confirmed more kidney fibrosis in myeloid COX-2<sup>-/-</sup> mice than WT mice (Fig. 2 D-E).

#### **Myeloid COX-2-derived PGE2 regulated renal myeloid cell polarization via EP4 receptors.**

To determine the prostanoid profile derived from COX-2 enzymatic activity in myeloid cells (Fig. 3A), we isolated BMDMs from WT and global COX-2<sup>-/-</sup> mice, incubated them in the presence of arachidonic acid for 1 h, and then determined prostanoids released into the medium using GC/MS<sup>13,20</sup>. The major prostanoid derived from COX-2 was PGE2 since it was the only prostanoid with decreased production in COX-2<sup>-/-</sup> BMDMs (Fig. 3B). PGE2 acts via PGE2 receptors EP1-EP4. To determine which PGE2 receptor modulated myeloid cell inflammatory response, isolated BMDMs were polarized to an “M1” (via LPS/IFN- $\gamma$ ) or “M2” (via IL-4/IL-13) phenotype. BMDMs expressed detectable *Ptger2*, *Ptger3* and *Ptger4* mRNA but only *Ptger4* mRNA expression changed in response to either M1 or M2 polarization (Fig. 3C).

EP4 was also the major PGE2 receptor subtype in the mouse macrophage-like cell line, RAW264.7<sup>20</sup>. PGE2-mediated inhibition of proinflammatory *Tnf* expression and stimulation of antiinflammatory *Arg1* expression in these cells were blocked by the selective EP4 receptor antagonist, L161982, but not by the selective EP2 receptor antagonist, PF04418948 (Fig. 3D).

We generated myeloid EP4<sup>-/-</sup> mice (CD11b-Cre; EP4<sup>fl/fl</sup>) mice to evaluate the possible role of EP4 receptors in myeloid COX-2-mediated renal myeloid cell polarization. Three days after ischemic injury, myeloid EP4<sup>-/-</sup> mice had increased renal myeloid populations and increased renal myeloid proinflammatory cytokines such as *Tnf*, *Ccl3*, *Il1a*, and *Il23a* (Fig. 3E), similar the responses in myeloid COX-2<sup>-/-</sup> mouse kidneys. Myeloid EP4<sup>-/-</sup> mouse kidneys also had increased macrophages and fibrosis four weeks after ischemic injury (Fig. 3F).

### COX-2/PGE2/EP4 signaling regulated expression of MafB, a master transcription factor for macrophage pro-resolving polarization.

EP4 receptors couple to G<sub>s</sub> and stimulate adenylyl cyclase (AC) to activate the cAMP/PKA/CREB pathway and Epac, a guanine nucleotide exchange factor for Rap<sup>22,23</sup>. The cell permeable cAMP analog dibutyryl-cAMP (db-cAMP) treatment inhibited *Tnf* expression and stimulated *Arg1* expression in RAW264.7 cells, with reversal by either a selective PKA antagonist (H89) or CREB inhibitor (666-15) (Fig. 4 A-B) but not by an Epac inhibitor (data not shown).

CREB has been reported to mediate PGE2-induced macrophage M2 polarization<sup>24</sup>. MEME Suite motif-based sequence analysis tools (<http://meme-suite.org/>) did not identify any predicted conserved CREB binding sites at the promoters of PGE2-regulated *Arg1* and *Tgm2* genes. The basic leucine zipper transcription factor, MafB, is known to upregulate antiinflammatory genes and suppress proinflammatory genes<sup>25</sup>. We analyzed RNA-seq data from a public GEO database (GSE119521) of macrophages exposed to PGE2 and a gene set of MafB target genes from GSE75722<sup>26</sup> to perform Gene Set Enrichment Analysis (GSEA)<sup>27</sup> to determine whether an *a priori* MafB target gene set showed statistically significant concordant differences in BMDM with PGE2 treatment (See Methods and Table S1). GSEA indicated *Arg1* and *Tgm2* could be regulated by MafB in BMDMs treated with PGE2 (NES = 1.35, FDRq = 0.02) (Fig. 4C). Further analysis of GSE75722<sup>26</sup> indicated that in mouse BMDMs, MafB has the potential to directly bind promoters to inhibit proinflammatory genes (*Tnf*, *Ccl2*, *Ccl3*) and stimulate antiinflammatory genes (*Arg1*, *Tgm2*, *Cd206*, *Il10*) as well as the phagocytosis associated gene, *Tyro3* (Fig. S3)<sup>26</sup>. MafB can also bind to enhancers to downregulate other proinflammatory genes and upregulate other pro-resolving genes (Fig. S3).

In RAW264.7 cells transfected with a luciferase reporter construct of the proximal 1050 base pairs of the *Mafb* promoter, either PGE2 or the EP4 agonist CY10598 increased luciferase expression (Fig. 4D). Consistent with a previous report of a CREB binding site at -201 in the *Mafb* promoter<sup>28</sup>, increased luciferase expression induced by either PGE2 or the EP4 agonist was suppressed by CREB inhibition with 665-15 (Fig. 4D). PGE2, CAY10598 (EP4 agonist), or 6-Bnz-cAMP (PKA agonist) all increased *Mafb* expression in RAW264.7 cells (Fig. 4E). PGE2-induced *Mafb* expression was suppressed by inhibition of EP4 receptors but not EP2 receptors (Fig. 4F). In addition, either PKA or CREB inhibition abolished db-cAMP-induced *Mafb* mRNA expression (Fig. 4F). COX-2 and MafB co-localized in many renal macrophages in WT mouse kidneys 3 days after ischemic injury, but MafB was



undetectable in renal macrophages in both myeloid COX-2<sup>-/-</sup> mice and EP4<sup>-/-</sup> mice (Fig. 4 G-H).

### Myeloid MafB deletion resulted in renal inflammation and delayed renal functional recovery after severe ischemic injury.

To investigate the role of myeloid MafB in the response of myeloid COX-2/PGE2/EP4 deletion, we generated mice with myeloid Mafb deletion (LysM-Cre; Mafb<sup>f/f</sup>; myeloid Mafb<sup>-/-</sup>). Myeloid Mafb deletion was confirmed by 10 times lower *Mafb* mRNA levels in BMDMs and renal myeloid cells isolated from myeloid Mafb<sup>-/-</sup> mice (Fig. S4A). Immunofluorescent staining confirmed MafB deletion in renal macrophages in myeloid Mafb<sup>-/-</sup> mice (Fig. S4B). Mafb<sup>-/-</sup> BMDMs had augmented LPS/IFN- $\gamma$ -induced proinflammatory *Tnf* and *Nos2* stimulation and decreased IL-4/IL-13-induced antiinflammatory *Arg1* and *Tgm2* expression (Fig. S4C). Inhibition of proinflammatory TNF- $\alpha$  and stimulation of antiinflammatory ARG1 by either PGE2 or a EP4 receptor agonist were markedly attenuated in Mafb<sup>-/-</sup> BMDMs (Fig. S4D) and in RAW264.7 cells following stable Mafb knockout (Mafb  $\Delta$ ) (Fig. S4E).

Similar to what was seen in myeloid COX-2<sup>-/-</sup> mice, there was no difference from wild type in the initial response to ischemic injury in myeloid Mafb<sup>-/-</sup> mice, but functional recovery was delayed in myeloid Mafb<sup>-/-</sup> mice (Fig. 5A). Three days after ischemic injury, myeloid Mafb<sup>-/-</sup> mice had increased renal myeloid populations (Fig. 5B) and increased renal myeloid proinflammatory cytokine expression (Fig. 5C), as well as higher kidney TNF- $\alpha$  levels (Fig. 5D). Similar to myeloid cell COX-2 deletion, myeloid cell Mafb<sup>-/-</sup> deletion also led to impaired efferocytosis (Fig. S5). Additionally, 4 weeks after ischemic injury, myeloid Mafb<sup>-/-</sup> mice developed more renal tubulointerstitial fibrosis, indicated by quantitative Sirius red staining,  $\alpha$ -SMA and collagen I immunostaining, and collagen IV and  $\alpha$ -SMA immunoblotting (Fig. 5 E-F).

### EP4 activation rescued the abnormalities induced by myeloid COX-2 deletion.

Unilateral ureteral obstruction (UUO) induces inflammatory injury and rapid development of progressive tubulointerstitial fibrosis, thereby providing an effective and convenient model for studying pharmacological rescue. Renal myeloid *Ptgs2* and *Mafb* expression increased after UUO (Fig. 6A). Both myeloid COX-2<sup>-/-</sup> mice and myeloid Mafb<sup>-/-</sup> mice and their WT controls were subjected to UUO for 7 days with or without administration of the EP4 agonist (ONO-4819) to the mice with gene deletion. In COX-2<sup>-/-</sup> mice, the EP4 agonist significantly increased myeloid MafB expression and decreased renal macrophages, myeloid proinflammatory cytokine expression, and renal fibrosis (Fig. 6 B-G). In contrast, the EP4 agonist did not rescue any of these abnormalities in Mafb<sup>-/-</sup> mice exposed to UUO (Fig. 6H and Fig. S6). We further investigated whether EP4 activation rescued renal functional recovery in ischemic injury in myeloid COX-2<sup>-/-</sup> mice and myeloid MafB<sup>-/-</sup> mice. EP4 activation rescued functional recovery in myeloid COX-2<sup>-/-</sup> mice but not MafB<sup>-/-</sup> mice (Fig. S7). Of note, EP4 activation had a trend to facilitate renal functional recovery in WT mice (Fig. S7).

## Discussion

Previous studies in the kidney have focused on intrinsic COX-2 expression and function<sup>29–43</sup>. However, the potential role of renal myeloid COX-2 in response to development of renal interstitial fibrosis as a sequela to acute injury has not been previously investigated. The current studies demonstrated: 1) COX-2 selectively increased in renal macrophages after AKI; 2) mice with myeloid COX-2 deletion had increased injury, delayed recovery, persistent proinflammatory renal macrophages, and increased tubulointerstitial fibrosis following AKI; 3) PGE2 was the major myeloid COX-2 metabolite and acted via activation of EP4 receptors to inhibit proinflammatory cytokines and promote antiinflammatory cytokines *in vitro*; 4) myeloid EP4 deletion mimicked the abnormalities seen with myeloid COX-2 deletion in response to AKI; 5) myeloid cell EP4 activation upregulated MafB expression *in vitro* and *in vivo*; and myeloid MafB deletion recapitulated abnormalities seen with myeloid COX-2 or EP4 deletion; and 6) EP4 activation rescued the abnormalities induced by myeloid COX-2 deletion but not by myeloid MafB deletion.

Our studies identify a mechanism by which COX-2 dependent EP4 activation mediates macrophage polarization to an antiinflammatory and pro-resolving phenotype. PGE2 or selective EP4 agonists increased expression of pro-resolving markers. EP4 is known to signal primarily through G<sub>s</sub>-coupled activation of adenylate cyclase, with production of cAMP and activation of PKA, and cAMP or a PKA agonist mimicked the effect of PGE2 and EP4 activation, while a PKA antagonist or a CREB inhibitor blocked such effects.

MafB is a transcription factor of the large Maf subfamily that contains MafA, MafB, c-Maf, and Nrl and is characterized by the presence of a transactivation domain in the N-terminal region and C-terminal basic leucine-zipper DNA-binding domain. Recent studies have indicated that MafB plays crucial roles in macrophage function, particularly in their polarization into a pro-resolving phenotype<sup>25,26,44–47</sup>. However, its role in COX-2/PGE2/EP4-mediated macrophage polarization has not been previously investigated. PGE2 and EP4 stimulated macrophage MafB expression, and myeloid MafB deletion prevented PGE2 and EP4 induction of pro-resolving macrophage polarization. Although administration of an EP4 agonist was able to ameliorate development of renal fibrosis in mice with myeloid COX-2 deletion, it had no effect in mice with myeloid MafB deletion. Collectively, these studies describe a heretofore undescribed mechanism by which macrophage COX-2-dependent PGE2 production acts in an autocrine and/or paracrine fashion to activate EP4, thereby stimulating expression of MafB, which mediates macrophage polarization to an antiinflammatory and pro-resolving phenotype. Although it is well established that alternatively activated (“M2”) macrophages can not only promote tissue repair but also mediate increased fibrosis in pathologic conditions, it is also recognized that persistent, unresolved inflammation can lead to epithelial cell dedifferentiation and G2/M arrest, resulting in production of profibrotic factors that induce myofibroblast transformation and production of collagens and other extracellular matrix components<sup>48</sup>.

Neutrophils are the first cells to enter the post-ischemic kidney and quickly undergo apoptosis. It is then the job of the pro-resolution macrophages to clear them by efferocytosis. Macrophages are also necessary for phagocytosis of damaged and apoptotic epithelial

cells after AKI. Compared to wild type mice following ischemic injury, mice with myeloid COX-2 deficiency had persistent renal neutrophil infiltration. *Ex vivo* studies demonstrated that COX-2-deficient renal macrophages from post-ischemic kidneys had decreased efferocytotic capacity. In addition, flow cytometry analysis demonstrated that BMDMs with either COX-2 or Mafk deficiency had impaired ability to phagocytose apoptotic neutrophils.

In addition to regulation of myeloid polarization, myeloid -derived PGE<sub>2</sub> may also bind to EP4 in adjacent non-myeloid cells. It has been reported that vascular EP4 receptors protect against angiotensin II-induced kidney damage<sup>49,50</sup>, collecting duct EP4 receptors regulate urine concentrating ability through increased aquaporin 2 expression and membrane targeting<sup>51</sup>, and EP4 receptors in tubular epithelial cells inhibit the loss of mitochondria in ischemic renal injury<sup>52</sup>.

In summary, these studies demonstrate an important role for myeloid-derived COX-2 and its enzymatic product, PGE<sub>2</sub> in mediation of recovery from acute kidney injury and prevention of the development of progressive tubulointerstitial fibrosis and identify new mechanisms underlying the polarization to a pro-resolving macrophage phenotype. In correlative analysis in human kidney diseases, examination of the Nephroseq database (<http://www.nephroseq.org/>) indicates that PTGS2 (COX-2) expression was decreased in the kidney glomerulus in patients in chronic kidney disease, in the tubulointerstitial compartment in minimal change disease, and in blood cells in IgA nephropathy (Fig. S8). Furthermore, the detrimental effects of NSAID use in the setting of kidney disease are well-documented. Although classical teaching suggests afferent arteriolar vasoconstriction to be the predominant underlying mechanism promoting or exacerbating injury, the current study identifies an additional, previously unknown mechanism by which myeloid COX-2 inhibition exacerbates acute and chronic kidney injury, a finding that is relevant to understanding the potential detrimental effects of NSAIDs in the setting of renal dysfunction.

## Supplementary Material

Refer to Web version on PubMed Central for supplementary material.

## Acknowledgments

### Funding:

These studies were supported by NIH grants, DK51265, DK95785, DK62794, P30DK114809 (RCH, MZZ), VA Merit Award 00507969 (RCH), the Vanderbilt Center for Kidney Disease, and National Natural Science Foundation of China 81870490 (YP).

## REFERENCES

1. Devarajan P. Emerging urinary biomarkers in the diagnosis of acute kidney injury. *Expert Opin Med Diagn* 2008; 2: 387–98. [PubMed: 19079800]
2. Zhang MZ, Yao B, Yang S, et al. CSF-1 signaling mediates recovery from acute kidney injury. *J Clin Invest* 2012; 122: 4519–32. [PubMed: 23143303]

3. Lever JM, Hull TD, Boddu R, et al. Resident macrophages reprogram toward a developmental state after acute kidney injury. *JCI Insight* 2019; 4: e125503
4. George JF, Lever JM, Agarwal A. Mononuclear phagocyte subpopulations in the mouse kidney. *Am J Physiol Renal Physiol* 2017; 312: F640–F6. [PubMed: 28100500]
5. Wang X, Yao B, Wang Y, et al. Macrophage Cyclooxygenase-2 Protects Against Development of Diabetic Nephropathy. *Diabetes* 2017; 66: 494–504. [PubMed: 27815317]
6. Nataraj C, Thomas DW, Tilley SL, et al. Receptors for prostaglandin E(2) that regulate cellular immune responses in the mouse. *J Clin Invest* 2001; 108: 1229–35. [PubMed: 11602631]
7. Takayama K, Garcia-Cardena G, Sukhova GK, et al. Prostaglandin E2 Suppresses Chemokine Production in Human Macrophages through the EP4 Receptor. *J Biol Chem* 2002; 277: 44147–54. [PubMed: 12215436]
8. Tang EH, Shvartz E, Shimizu K, et al. Deletion of EP4 on bone marrow-derived cells enhances inflammation and angiotensin II-induced abdominal aortic aneurysm formation. *Arterioscler Thromb Vasc Biol* 2011; 31: 261–9. [PubMed: 21088251]
9. Schneider A, Guan Y, Zhang Y, et al. Generation of a conditional allele of the mouse prostaglandin EP4 receptor. *Genesis* 2004; 40: 7–14. [PubMed: 15354288]
10. Wang D, Patel VV, Ricciotti E, et al. Cardiomyocyte cyclooxygenase-2 influences cardiac rhythm and function. *Proc Natl Acad Sci U S A* 2009; 106: 7548–52. [PubMed: 19376970]
11. Ferron M, Vacher J. Targeted expression of Cre recombinase in macrophages and osteoclasts in transgenic mice. *Genesis* 2005; 41: 138–45. [PubMed: 15754380]
12. Sasaki K, Terker AS, Pan Y, et al. Deletion of Myeloid Interferon Regulatory Factor 4 (Irf4) in Mouse Model Protects against Kidney Fibrosis after Ischemic Injury by Decreased Macrophage Recruitment and Activation. *J Am Soc Nephrol* 2021; 32: 1037–52. [PubMed: 33619052]
13. Zhang MZ, Xu J, Yao B, et al. Inhibition of 11beta-hydroxysteroid dehydrogenase type II selectively blocks the tumor COX-2 pathway and suppresses colon carcinogenesis in mice and humans. *J Clin Invest* 2009; 119: 876–85. [PubMed: 19307727]
14. Zhang MZ, Yao B, Wang S, et al. Intrarenal dopamine deficiency leads to hypertension and decreased longevity in mice. *J Clin Invest* 2011; 121: 2845–54. [PubMed: 21701066]
15. Moore JF, Sharer JD. Methods for Quantitative Creatinine Determination. *Curr Protoc Hum Genet* 2017; 93: A 30 1–A 30 7.
16. Langmead B, Wilks C, Antonescu V, Charles R. Scaling read aligners to hundreds of threads on general-purpose processors. *Bioinformatics* 2019; 35: 421–32. [PubMed: 30020410]
17. Feng J, Liu T, Qin B, et al. Identifying ChIP-seq enrichment using MACS. *Nat Protoc* 2012; 7: 1728–40. [PubMed: 22936215]
18. Robinson JT, Thorvaldsdottir H, Winckler W, et al. Integrative genomics viewer. *Nat Biotechnol* 2011; 29: 24–6. [PubMed: 21221095]
19. Subramanian A, Tamayo P, Mootha VK, et al. Gene set enrichment analysis: a knowledge-based approach for interpreting genome-wide expression profiles. *Proc Natl Acad Sci U S A* 2005; 102: 15545–50. [PubMed: 16199517]
20. Zhang MZ, Yao B, Wang Y, et al. Inhibition of cyclooxygenase-2 in hematopoietic cells results in salt-sensitive hypertension. *J Clin Invest* 2015; 125: 4281–94. [PubMed: 26485285]
21. Zhong X, Lee HN, Kim SH, et al. Myc-nick promotes efferocytosis through M2 macrophage polarization during resolution of inflammation. *Faseb J* 2018; 32: 5312–25. [PubMed: 29718706]
22. Yokoyama U, Iwatsubo K, Umemura M, et al. The prostanoid EP4 receptor and its signaling pathway. *Pharmacol Rev* 2013; 65: 1010–52. [PubMed: 23776144]
23. Nakatsuji M, Minami M, Seno H, et al. EP4 Receptor-Associated Protein in Macrophages Ameliorates Colitis and Colitis-Associated Tumorigenesis. *PLoS Genet* 2015; 11: e1005542. [PubMed: 26439841]
24. Luan B, Yoon YS, Le Lay J, et al. CREB pathway links PGE2 signaling with macrophage polarization. *Proc Natl Acad Sci U S A* 2015; 112: 15642–7. [PubMed: 26644581]
25. Kim H. The transcription factor MafB promotes anti-inflammatory M2 polarization and cholesterol efflux in macrophages. *Sci Rep* 2017; 7: 7591. [PubMed: 28790455]

26. Soucie EL, Weng Z, Geirsdottir L, et al. Lineage-specific enhancers activate self-renewal genes in macrophages and embryonic stem cells. *Science* 2016; 351: aad5510. [PubMed: 26797145]
27. Sanin DE, Matsushita M, Klein Geltink RI, et al. Mitochondrial Membrane Potential Regulates Nuclear Gene Expression in Macrophages Exposed to Prostaglandin E2. *Immunity* 2018; 49: 1021–33 e6. [PubMed: 30566880]
28. Zhang X, Odom DT, Koo SH, et al. Genome-wide analysis of cAMP-response element binding protein occupancy, phosphorylation, and target gene activation in human tissues. *Proc Natl Acad Sci U S A* 2005; 102: 4459–64. [PubMed: 15753290]
29. Harris RC, McKanna JA, Akai Y, et al. Cyclooxygenase-2 is associated with the macula densa of rat kidney and increases with salt restriction. *J Clin Invest* 1994; 94: 2504–10. [PubMed: 7989609]
30. Zhang MZ. Interaction of renal cortical cyclooxygenase-2 and angiotensin II in postnatal nephrogenesis. *Kidney Int* 2017; 91: 771–3. [PubMed: 28314575]
31. Cheng HF, Wang JL, Zhang MZ, et al. Role of p38 in the regulation of renal cortical cyclooxygenase-2 expression by extracellular chloride. *J Clin Invest* 2000; 106: 681–8. [PubMed: 10974021]
32. Zhang MZ, Hao CM, Breyer MD, et al. Mineralocorticoid regulation of cyclooxygenase-2 expression in rat renal medulla. *Am J Physiol Renal Physiol* 2002; 283: F509–16. [PubMed: 12167602]
33. Zhang MZ, Harris RC, McKanna JA. Regulation of cyclooxygenase-2 (COX-2) in rat renal cortex by adrenal glucocorticoids and mineralocorticoids. *Proc Natl Acad Sci U S A* 1999; 96: 15280–5. [PubMed: 10611376]
34. Cheng HF, Wang JL, Zhang MZ, et al. Angiotensin II attenuates renal cortical cyclooxygenase-2 expression. *J Clin Invest* 1999; 103: 953–61. [PubMed: 10194467]
35. Zhang MZ, Wang JL, Cheng HF, et al. Cyclooxygenase-2 in rat nephron development. *Am J Physiol* 1997; 273: F994–1002. [PubMed: 9435689]
36. Zhang MZ, Sanchez Lopez P, McKanna JA, Harris RC. Regulation of cyclooxygenase expression by vasopressin in rat renal medulla. *Endocrinology* 2004; 145: 1402–9. [PubMed: 14684611]
37. Jensen BL, Kurtz A. Differential regulation of renal cyclooxygenase mRNA by dietary salt intake. *Kidney Int* 1997; 52: 1242–9. [PubMed: 9350647]
38. Frolich S, Slattery P, Thomas D, et al. Angiotensin II-AT1-receptor signaling is necessary for cyclooxygenase-2-dependent postnatal nephron generation. *Kidney Int* 2017; 91: 818–29. [PubMed: 28040266]
39. Francois H, Coffman TM. Prostanoids and blood pressure: which way is up? *J Clin Invest* 2004; 114: 757–9. [PubMed: 15372097]
40. Dinchuk JE, Car BD, Focht RJ, et al. Renal abnormalities and an altered inflammatory response in mice lacking cyclooxygenase II. *Nature* 1995; 378: 406–9. [PubMed: 7477380]
41. Komers R, Lindsley JN, Oyama TT, et al. Immunohistochemical and functional correlations of renal cyclooxygenase-2 in experimental diabetes. *J Clin Invest* 2001; 107: 889–98. [PubMed: 11285308]
42. Yang T, Sun D, Huang YG, et al. Differential regulation of COX-2 expression in the kidney by lipopolysaccharide: role of CD14. *Am J Physiol* 1999; 277: F10–6. [PubMed: 10409292]
43. Park JM, Yang T, Arend LJ, et al. Obstruction stimulates COX-2 expression in bladder smooth muscle cells via increased mechanical stretch. *Am J Physiol* 1999; 276: F129–36. [PubMed: 9887088]
44. Aziz A, Soucie E, Sarrazin S, Sieweke MH. MafB/c-Maf deficiency enables self-renewal of differentiated functional macrophages. *Science* 2009; 326: 867–71. [PubMed: 19892988]
45. Sarrazin S, Mossadegh-Keller N, Fukao T, et al. MafB restricts M-CSF-dependent myeloid commitment divisions of hematopoietic stem cells. *Cell* 2009; 138: 300–13. [PubMed: 19632180]
46. Tran MTN, Hamada M, Jeon H, et al. MafB is a critical regulator of complement component C1q. *Nat Commun* 2017; 8: 1700. [PubMed: 29167450]
47. Sato Y, Tsukaguchi H, Morita H, et al. A mutation in transcription factor MAFB causes Focal Segmental Glomerulosclerosis with Duane Retraction Syndrome. *Kidney Int* 2018; 94: 396–407. [PubMed: 29779709]

48. Yang L, Besschetnova TY, Brooks CR, et al. Epithelial cell cycle arrest in G2/M mediates kidney fibrosis after injury. *Nat Med* 2010; 16: 535–43. [PubMed: 20436483]
49. Thibodeau JF, Holterman CE, He Y, et al. Vascular Smooth Muscle-Specific EP4 Receptor Deletion in Mice Exacerbates Angiotensin II-Induced Renal Injury. *Antioxid Redox Signal* 2016; 25: 642–56. [PubMed: 27245461]
50. Xu H, Du S, Fang B, et al. VSMC-specific EP4 deletion exacerbates angiotensin II-induced aortic dissection by increasing vascular inflammation and blood pressure. *Proc Natl Acad Sci U S A* 2019; 116: 8457–62. [PubMed: 30948641]
51. Gao M, Cao R, Du S, et al. Disruption of prostaglandin E2 receptor EP4 impairs urinary concentration via decreasing aquaporin 2 in renal collecting ducts. *Proc Natl Acad Sci U S A* 2015; 112: 8397–402. [PubMed: 26100911]
52. Ding C, Han F, Xiang H, et al. Role of prostaglandin E2 receptor 4 in the modulation of apoptosis and mitophagy during ischemia/reperfusion injury in the kidney. *Mol Med Rep* 2019; 20: 3337–46. [PubMed: 31432142]



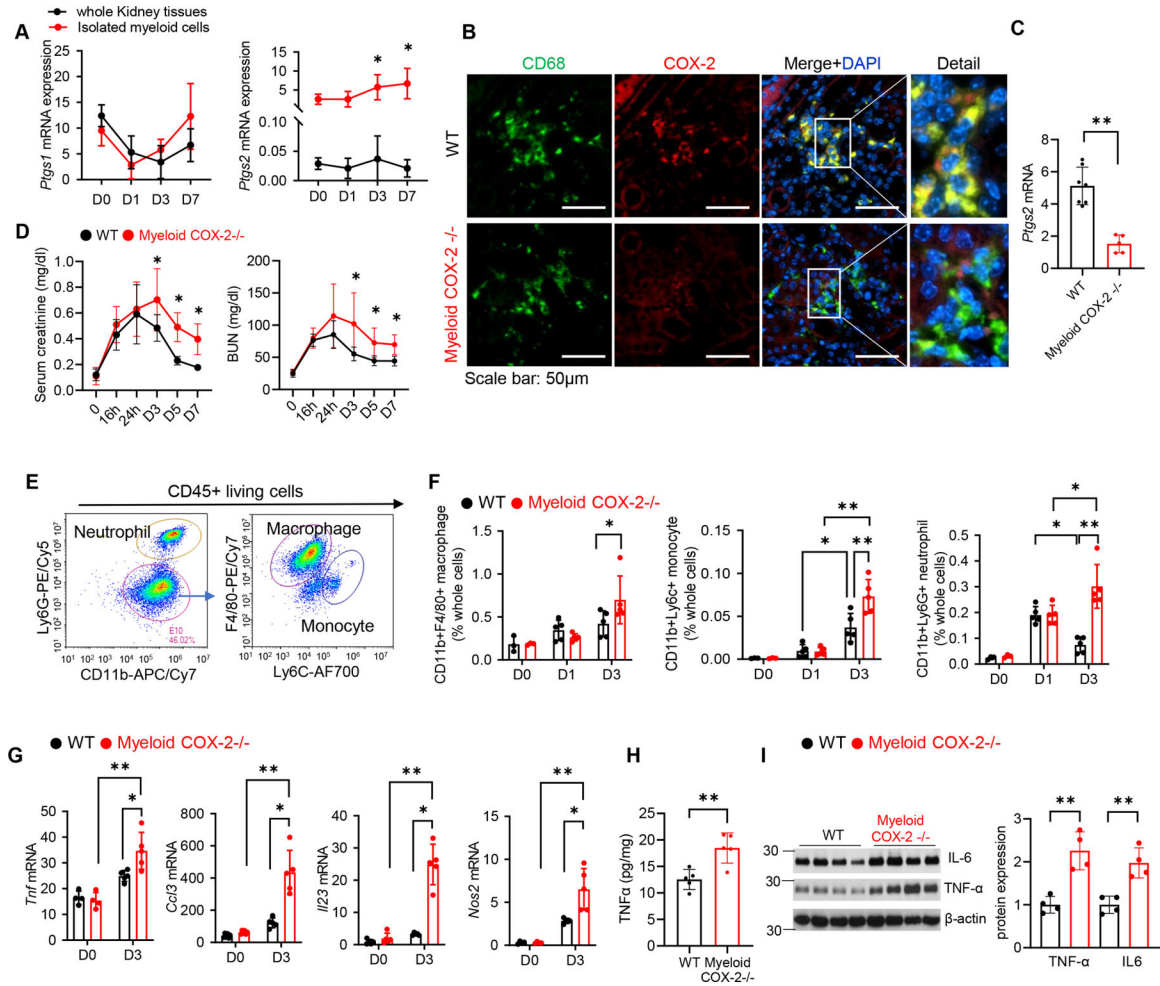


**Fig. 1. Selective COX-2 deletion in myeloid cells led to delayed renal functional recovery and renal myeloid cell proinflammatory polarization after ischemic AKI.**

(A) In WT mice, *Ptgs1* mRNA expression in kidneys and in renal myeloid cells was decreased after injury before returning toward baseline by day 7; *Ptgs2* mRNA expression was 100-fold higher in renal myeloid cells than in kidney and increased by day 3 after ischemic injury. \* $P < 0.05$  vs. day 0,  $n = 5$  at each time point. Data are means  $\pm$  SD, analyzed using 2-way ANOVA followed by Tukey's post hoc test. (B) Representative image show at three days after ischemic injury, COX-2 (red) was expressed in most renal CD68<sup>+</sup> macrophages (green) in WT mice but in only a small portion of renal macrophages in myeloid COX-2<sup>-/-</sup> mice. Scale bar = 50 $\mu$ m. (C) Renal myeloid cell *Ptgs2* mRNA expression was decreased >70% in myeloid COX-2<sup>-/-</sup> mice compared to WT mice cells 3 days after AKI. \*\* $P < 0.01$ ,  $n = 7$  in WT mice,  $n = 5$  in myeloid COX-2<sup>-/-</sup> mice. Data are means  $\pm$  SD, analyzed using 2-tailed Student's *t* test. (D) Myeloid COX-2<sup>-/-</sup> mice had similar initial injury compared to WT mice but had delayed functional recovery after injury. \* $P < 0.05$ ,  $n = 5$  at each time point per group. Data are means  $\pm$  SD, analyzed using 2-way ANOVA followed by Tukey's post hoc test. (E and F) Using gating strategy shown in (E), flow cytometry determined from day 1 to day 3 after ischemic injury, WT mouse kidney had decreased CD45<sup>+</sup>CD11b<sup>+</sup>Ly6G<sup>+</sup> neutrophils but persistently higher CD45<sup>+</sup>CD11b<sup>+</sup>F4/80<sup>+</sup>

macrophages and continuously increased CD45<sup>+</sup>CD11b<sup>+</sup>Ly6C<sup>+</sup> monocytes while all these cell populations increased in myeloid COX-2<sup>-/-</sup> mice. \**P*<0.05, \*\**P*<0.01, n=5 each time point per group. Data are means ± SD, analyzed using 2-way ANOVA followed by Tukey's post hoc test. (G) Renal myeloid cells of myeloid COX-2<sup>-/-</sup> mice had higher proinflammatory cytokine expression including *Tnf*, *Ccl3*, *Nos2*, and *Il23a* at day 3 after ischemic injury. \**P*<0.05, \*\**P*<0.01, n=5 at each time point per group. Data are means ± SD, analyzed using 2-way ANOVA followed by Bonferroni's post hoc tests. (H) ELISA indicated kidney TNF-α protein levels were higher in myeloid COX-2<sup>-/-</sup> mice than WT mice at day 3 after ischemic injury. \*\**P*<0.01, n=5. Data are means ± SD, analyzed using 2 tailed Student's t test. (I) Immunoblotting indicated higher IL-6 and TNF-α protein levels in myeloid COX-2<sup>-/-</sup> mice than WT mice. \*\**P*<0.01, n=4. Data are means ± SD, analyzed using 2 tailed Student's t test.

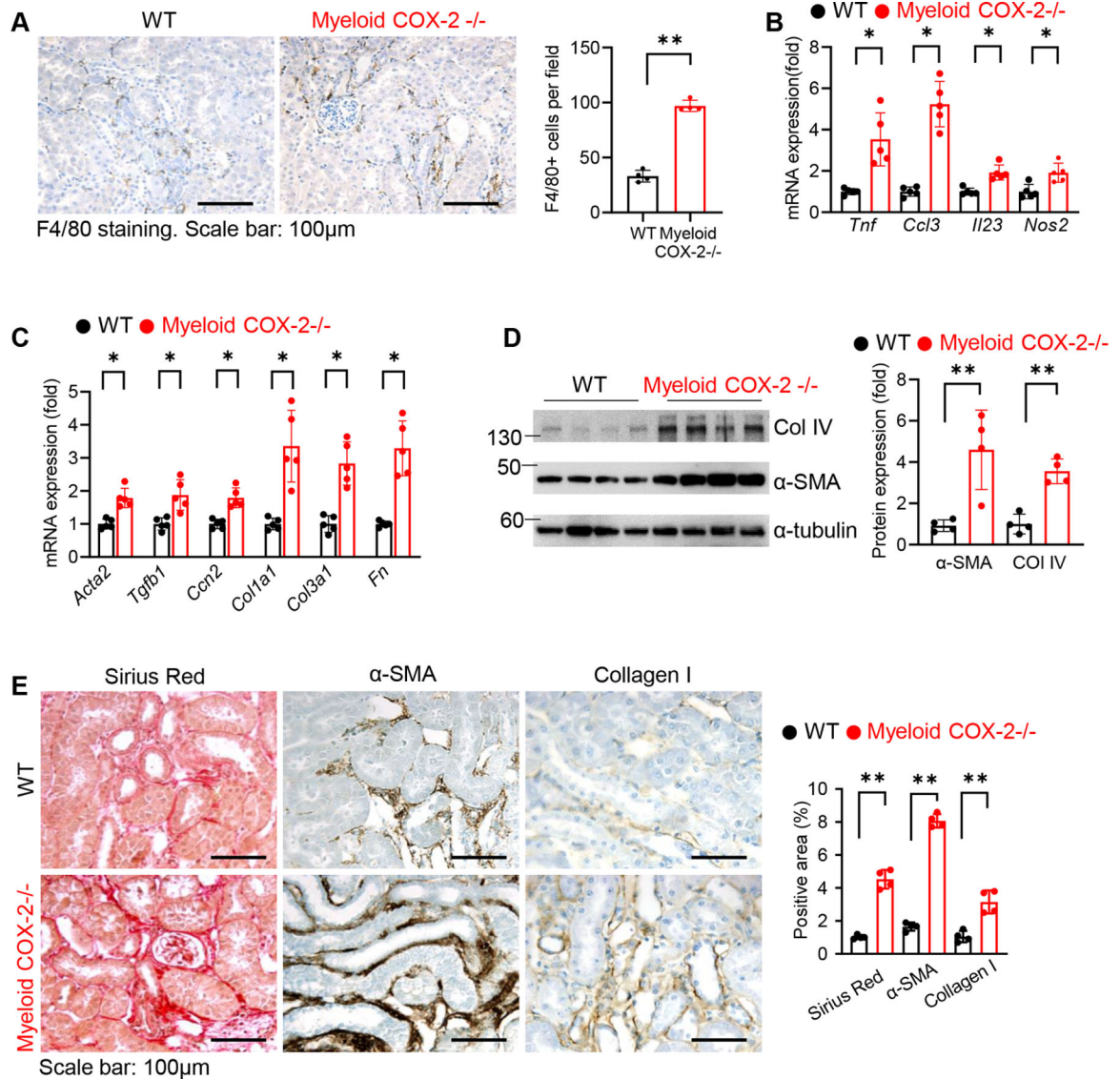


**Fig. 2. Myeloid COX-2<sup>-/-</sup> mouse kidney had more proinflammatory macrophages and robust fibrosis 4 weeks following ischemic injury.**

Both WT and myeloid COX-2<sup>-/-</sup> mice were subjected to ischemic injury for 4 weeks. (A) Myeloid COX-2<sup>-/-</sup> mice had more renal macrophages. \*\* $P$ <0.01,  $n$ =4. Data are means  $\pm$  SD, analyzed using 2 tailed Student's  $t$  test. Scale bar=100 $\mu$ m. (B) Myeloid COX-2<sup>-/-</sup> mice had increased renal myeloid cell mRNA levels of proinflammatory cytokines including *Nos2*, *Tnf*, *Ccl3*, and *Il23a*. \* $P$ <0.05,  $n$ =5. Data are means  $\pm$  SD, analyzed using 2-way ANOVA followed by Bonferroni's post hoc tests. (C) Myeloid COX-2<sup>-/-</sup> mouse kidney had higher mRNA expression of profibrotic and fibrotic components, including *Acta2*, *Tgfb1*, *Ccn2* (*Ctgf*), *Col1a1*, *Col3a1*, and *Fn*. \* $P$ <0.05,  $n$ =5. Data are means  $\pm$  SD, analyzed using 2-way ANOVA followed by Bonferroni's post hoc tests. (D and E) Immunoblotting (D) and quantitative Sirius red staining and  $\alpha$ -SMA and collagen I immunostaining (E) showed more renal interstitial fibrosis in myeloid COX-2<sup>-/-</sup> mice. \*\* $P$ <0.01,  $n$ =4. Data are means  $\pm$  SD, analyzed using 2-way ANOVA followed by Bonferroni's post hoc tests. Scale bar=100 $\mu$ m.

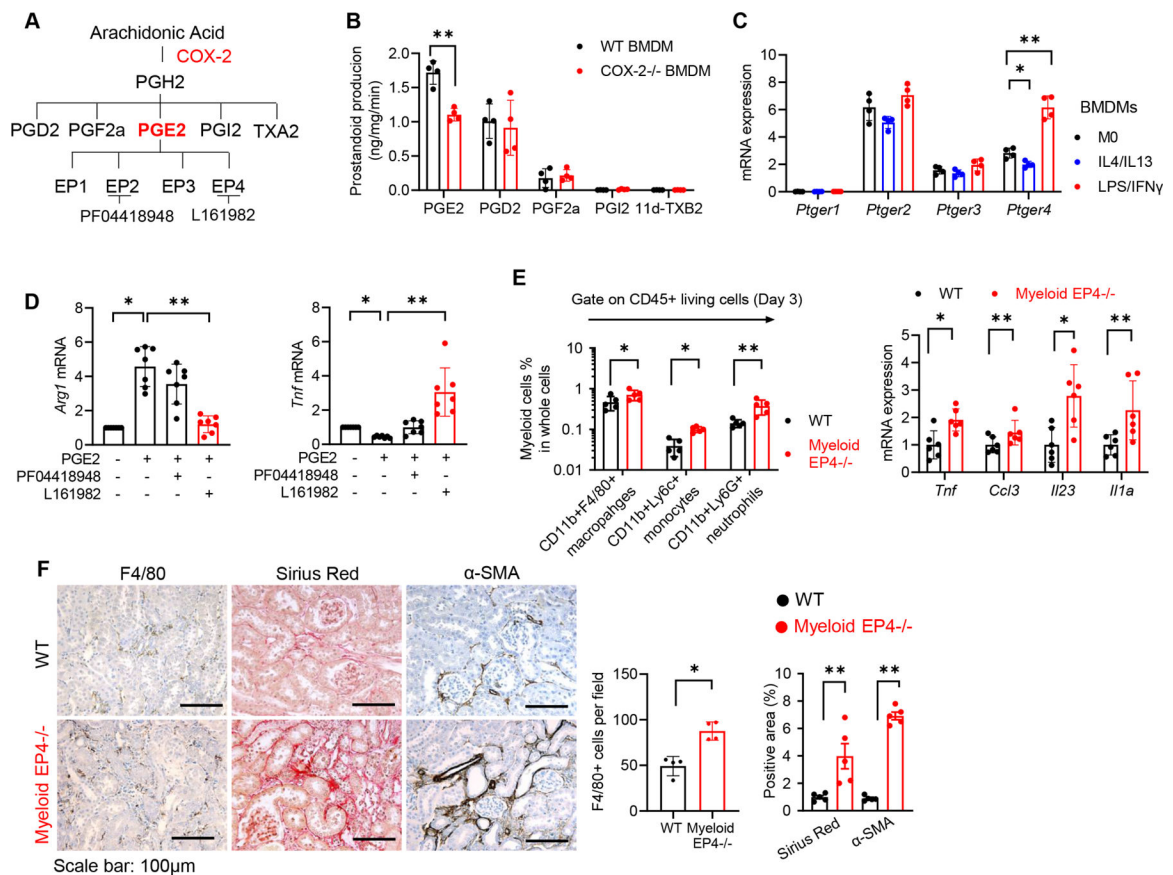


**Fig. 3. Myeloid COX-2-derived PGE2 regulated renal myeloid cell polarization via EP4 receptors.**

(A) Schematic diagram of COX2/PGE2/EP1–4 pathway. (B) COX-2<sup>-/-</sup> BMDMs isolated from global COX-2<sup>-/-</sup> mice produced less PGE2 compared to WT BMDMs. \*\* $P < 0.01$ ,  $n = 4$ . Data are means  $\pm$  SD, analyzed using 2-way ANOVA followed by Bonferroni's post hoc tests. (C) Among all detectable EP receptors, only *Ptger4* (EP4) mRNA expression was stimulated by M1 stimulation with LPS/IFN- $\gamma$  and inhibited by M2 stimulation with IL-4/IL-13 in BMDMs. \* $P < 0.05$ , \*\* $P < 0.01$ ,  $n = 4$  independent repeats. Data are means  $\pm$  SD, analyzed using 2-way ANOVA followed by Bonferroni's post hoc tests. (D) PGE2-mediated *Arg1* stimulation and *Tnf* inhibition in mouse RAW264.7 cells were reversed by the EP4 antagonist (L161982, 10  $\mu$ M) but not the EP2 antagonist (PF04418948, 10  $\mu$ M). \* $P < 0.05$ , \*\* $P < 0.01$ ,  $n = 6$  independent repeats. Data are means  $\pm$  SD, analyzed using 2-way ANOVA followed by Bonferroni's post hoc tests. (E) Myeloid EP4<sup>-/-</sup> mouse kidneys had increased renal CD45<sup>+</sup>CD11b<sup>+</sup>F4/80<sup>+</sup> macrophages, CD45<sup>+</sup>CD11b<sup>+</sup>Ly6c<sup>+</sup> monocytes, and CD45<sup>+</sup>CD11b<sup>+</sup>Ly6G<sup>+</sup> neutrophils determined by flow cytometry ( $n = 5$ ) as well as higher proinflammatory cytokine expression including *Tnf*, *Ccl3*, *Il23a*, and *Il1a* ( $n = 6$ ) at day 3 after ischemic injury. \* $P < 0.05$ , \*\* $P < 0.01$ . Data are means  $\pm$  SD, analyzed using 2-way ANOVA followed by Bonferroni's post hoc tests. (F) Sirius red staining and immunostaining demonstrated more renal macrophages and fibrosis in myeloid EP4<sup>-/-</sup> mice at week 4 after ischemic injury. \* $P < 0.05$ , \*\* $P < 0.01$ ,  $n = 4$ –5 mice per group. Data are means  $\pm$  SD, analyzed using 2 tailed Student's *t* test. Scale bar=100 $\mu$ m.



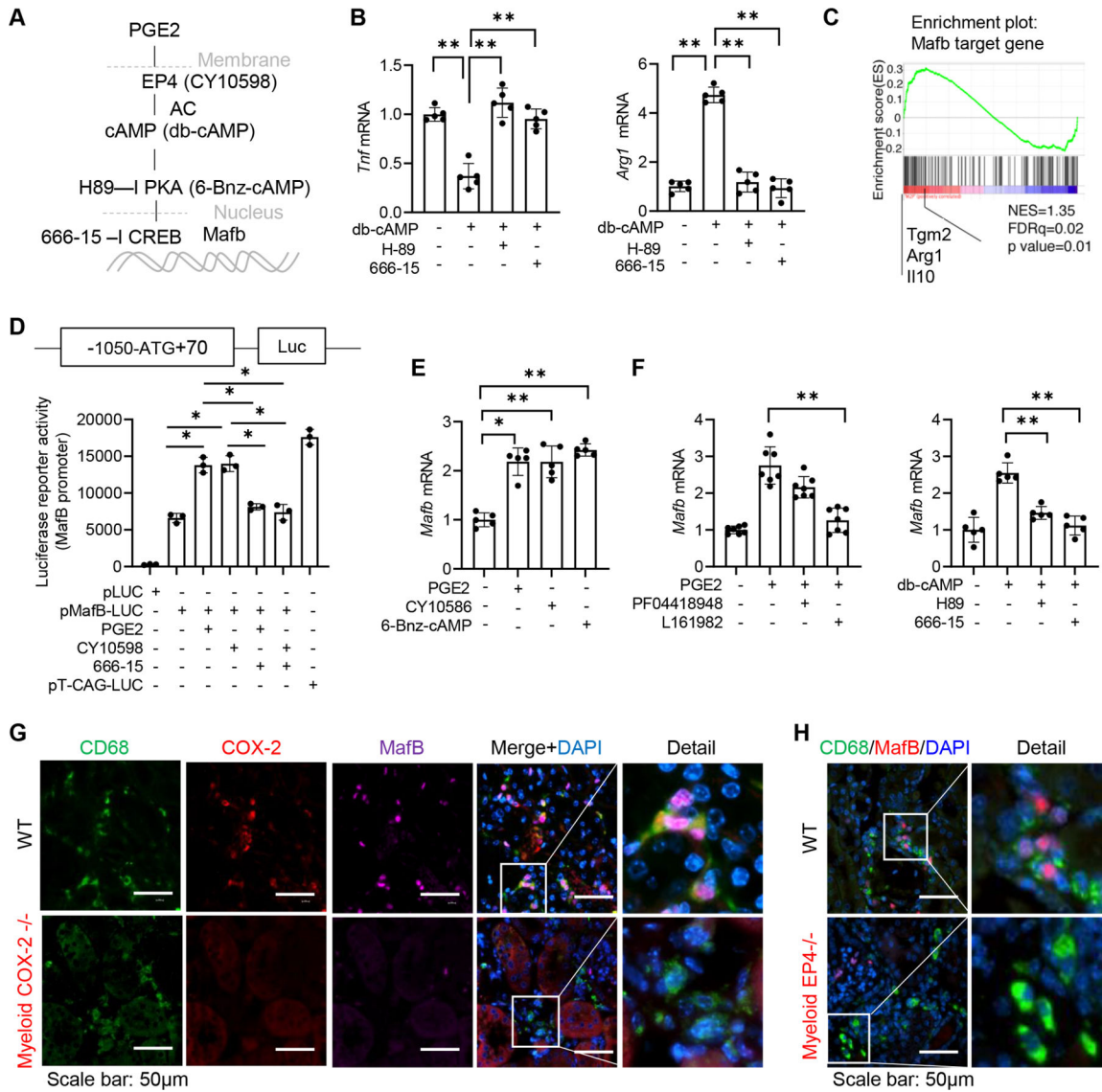


**Fig. 4. Transcription factor MafB mediated EP4-induced myeloid cell antiinflammatory and pro-resolving polarization.**

(A) Schematic diagram of PGE2/EP4/PKA/CREB/MafB pathway. (B) Inhibition of *Tnf* expression and stimulation of *Arg1* expression in RAW264.7 cells by a cell permeable cAMP analog, db-cAMP, were reversed by either PKA inhibition with H89 or CREB inhibition 666–15.  $**P < 0.01$ , n=5 independent repeats. Data are means  $\pm$  SD, analyzed using 2-way ANOVA followed by Bonferroni’s post hoc tests. (C) GSEA indicated that genes upregulated by PGE2, such as Arg1, Tgm2, and Il10 could be regulated by MafB in BMDMs (NES = 1.35, FDR q= 0.02). (D) Both PGE2 and EP4 agonist (CY10598) led to increased MafB promoter activity in a luciferase reporter assay, which was blocked by the CREB inhibitor (666–15).  $*P < 0.01$ , n=3 independent repeats. Data are means  $\pm$  SD, analyzed using 2-way ANOVA followed by Bonferroni’s post hoc tests. (E) BMDM *MafB* expression was stimulated by PGE2 or an EP4 agonist (CY10598) or a PKA agonist (6-Bnz-cAMP).  $*P < 0.05$ ,  $**P < 0.01$ , n=5 independent repeats. Data are means  $\pm$  SD, analyzed using

2-way ANOVA followed by Bonferroni's post hoc tests. (*F*) PGE2-induced *Mafb* expression was prevented by an EP4 antagonist (L161982) and the db-cAMP-induced *Mafb* expression was abolished by PKA inhibition with H-89 or CREB inhibition with 666-15. \*\* $P < 0.01$ ,  $n = 5-7$  independent repeats. Data are means  $\pm$  SD, analyzed using 2-way ANOVA followed by Bonferroni's post hoc tests. (*G* and *H*) Representative images showed COX-2 and MafB were colocalized to many renal macrophages in WT mice but was not detectable in renal macrophages in myeloid COX-2<sup>-/-</sup> mice (*G*) and in myeloid EP4<sup>-/-</sup> mice (*H*) 3 days after ischemic injury. Scale bar=50 $\mu$ m.

Author Manuscript

Author Manuscript

Author Manuscript

Author Manuscript



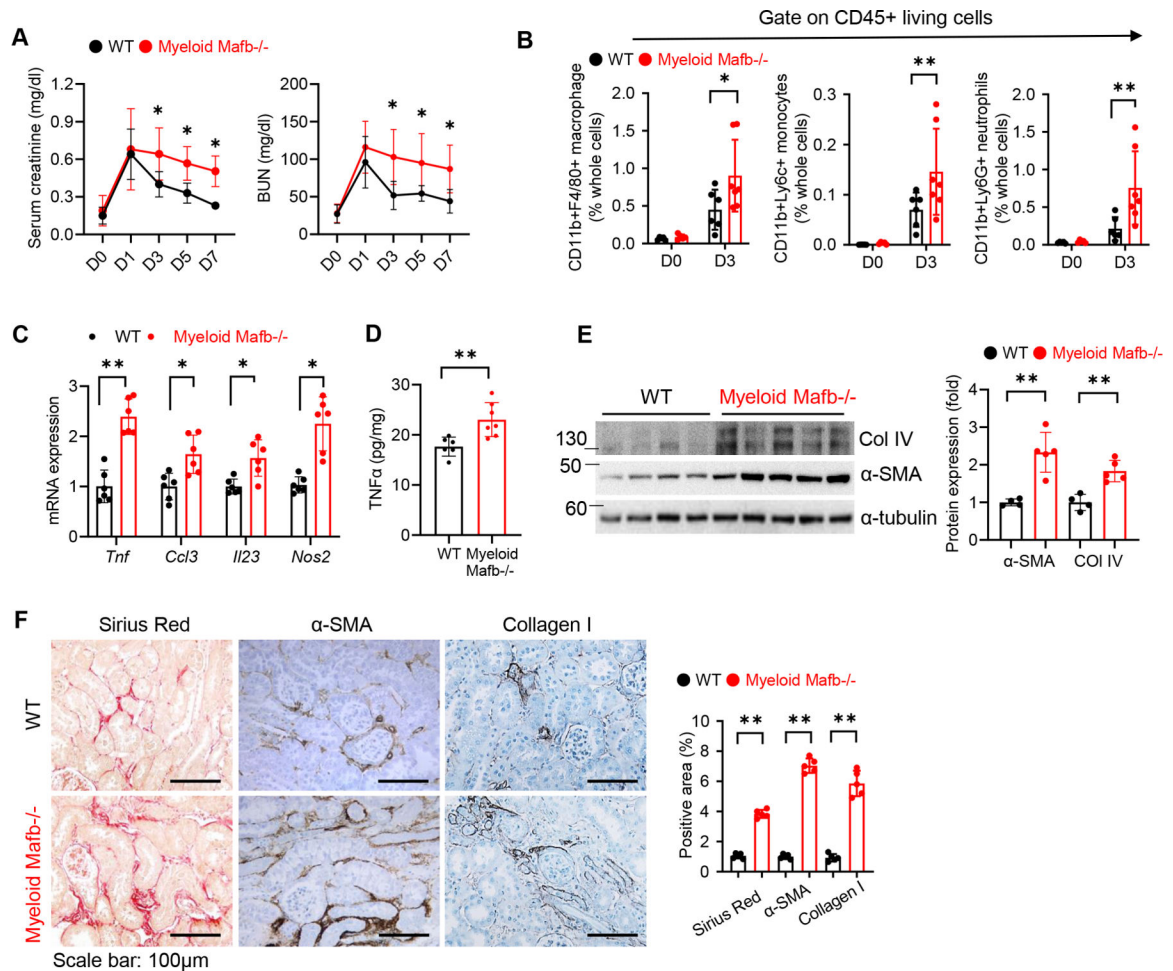


**Fig. 5. Myeloid *Mafb* deletion led to a delayed renal recovery, persistent proinflammatory macrophages, and robust fibrosis following ischemic injury.**

(A) Myeloid *Mafb*<sup>-/-</sup> mice had similar initial injury compared to WT mice but had delayed functional recovery after injury. \* $P < 0.05$ ,  $n = 8$  at each time point per group. Data are means  $\pm$  SD, analyzed using 2-way ANOVA followed by Tukey's post hoc test. (B) Flow cytometry analysis determined increased renal CD45<sup>+</sup>CD11b<sup>+</sup>F4/80<sup>+</sup> macrophages, CD45<sup>+</sup>CD11b<sup>+</sup>Ly6c<sup>+</sup> monocytes, and CD45<sup>+</sup>CD11b<sup>+</sup>Ly6G<sup>+</sup> neutrophils in myeloid *Mafb*<sup>-/-</sup> mice at day 3 after AKI. \* $P < 0.05$ , \*\* $P < 0.01$ ,  $n = 5$  at each time point per group. Data are means  $\pm$  SD, analyzed using 2-way ANOVA followed by Tukey's post hoc test. (C) Renal myeloid cells of myeloid *Mafb*<sup>-/-</sup> mice had higher proinflammatory cytokine expression including *Tnf*, *Ccl3*, *Il23a*, and *Nos2* at day 3 after ischemic injury. \* $P < 0.05$ , \*\* $P < 0.01$ ,  $n = 6$  at each time point per group. Data are means  $\pm$  SD, analyzed using 2-way ANOVA followed by Bonferroni's post hoc tests. (D) ELISA determined higher kidney TNF- $\alpha$  protein expression in myeloid *Mafb*<sup>-/-</sup> mice at day 3 following ischemic injury. \*\* $P < 0.01$ ,  $n = 7$ . Data are means  $\pm$  SD, analyzed using 2 tailed Student's t test. (E and F) Immunoblotting (E) and quantitative Sirius red staining and immunostaining (F) demonstrated more renal fibrosis in myeloid *Mafb*<sup>-/-</sup> mice than WT mice 4 weeks after ischemic injury. \*\* $P < 0.01$ ,  $n = 4-5$ . Data are means  $\pm$  SD, analyzed using 2 tailed Student's t test. Scale bar=100 $\mu$ m.

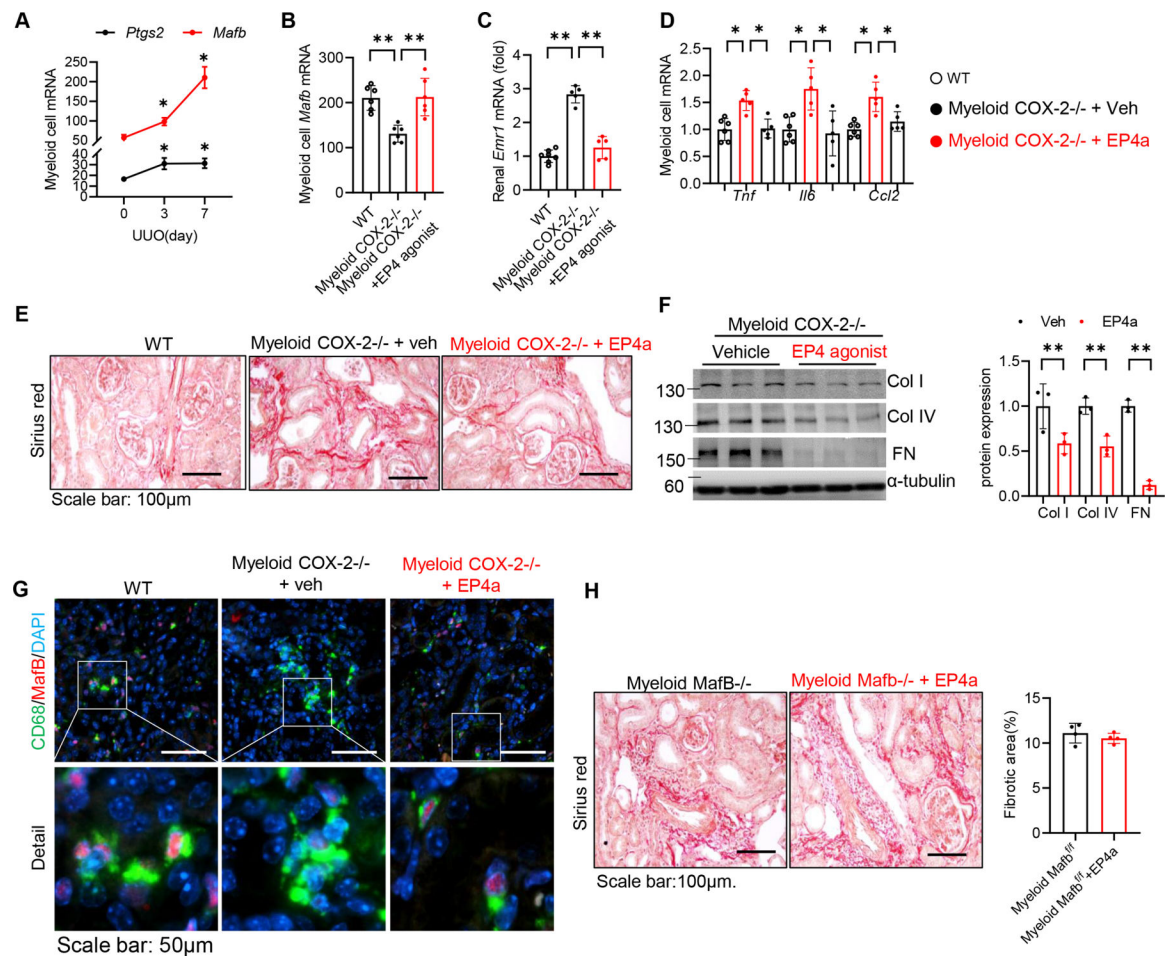


**Fig. 6. EP4 activation rescued abnormalities induced by myeloid COX-2 deletion but not by myeloid MafB deletion.**

Unilateral ureteral obstruction (UUO) was performed in both myeloid COX-2<sup>-/-</sup> mice and myeloid MafB<sup>-/-</sup> mice without or without administration of EP4 agonist, ONO-4819. (A) Both renal myeloid cell *Ptgs2* and *MafB* expression were increased after UUO. \* $P < 0.05$ ,  $n = 3-6$ . Data are means  $\pm$  SD, analyzed using 2-way ANOVA followed by Bonferroni's post hoc tests. (B and C) Decreased renal myeloid cell *MafB* expression (B) and increased kidney *Emr1* (F4/80) expression (C) in myeloid COX-2<sup>-/-</sup> mice after UUO for 7 days was reversed by EP4 agonist. \*\* $P < 0.01$ ,  $n = 5-7$ . Data are means  $\pm$  SD, analyzed using 2-way ANOVA followed by Bonferroni's post hoc tests. (D) EP4 activation attenuated increased renal myeloid cell proinflammatory cytokine expression in myeloid COX-2<sup>-/-</sup> mice after UUO for 7 days, including *Tnf*, *Il6*, and *Ccl2*. \* $P < 0.05$ ,  $n = 4-6$ . Data are means  $\pm$  SD, analyzed using 2-way ANOVA followed by Bonferroni's post hoc tests. (E) Sirius red staining showed that increased renal fibrosis in UUO myeloid COX-2<sup>-/-</sup> mice was attenuated by EP4 activation. Scale bar=100µm. (F) Immunoblotting illustrated that EP4 activation decreased kidney protein levels of collagen I (Col I), collagen IV (Col IV), and fibronectin (FN) in UUO myeloid COX-2<sup>-/-</sup> mice. \*\* $P < 0.05$ ,  $n = 3$ . Data are means  $\pm$  SD, analyzed using 2-way ANOVA followed by Bonferroni's post hoc tests. Scale bar=50µm. (G) EP4 activation increased renal macrophage MafB expression in myeloid COX-2<sup>-/-</sup>

mice after UUO. Scale bar=50 $\mu$ m. (H) EP4 activation did not affect renal fibrosis seen in myeloid Mafb<sup>-/-</sup> mice after UUO. N=5. Data are means  $\pm$  SD, analyzed using 2 tailed Student's t test. Scale bar=100 $\mu$ m.

Author Manuscript

Author Manuscript

Author Manuscript

Author Manuscript